Available online at www.sciencedirect.com
SCIENCE DIRECT
Polymer 47 (2006) 4816–4823
polymer
www.elsevier.com/locate/polymer

Thermooxidative stability of spectra of fluorene-based copolymers

Gui-Zhong Yang [a,b], Meng Wu [b], Su Lu [c], Min Wang [b], Tianxi Liu [a,b,*], Wei Huang [b]

[a] Key Laboratory of Molecular Engineering of Polymers of Chinese Ministry of Education, Department of Macromolecular Science, Fudan University, Shanghai 200433, People's Republic of China
[b] Laboratory of Advanced Materials, Fudan University, Shanghai 200433, People's Republic of China
[c] Institute of Materials Research and Engineering, National University of Singapore, 3 Research Link, Singapore 117602, Republic of Singapore

Received 9 December 2005; received in revised form 9 March 2006; accepted 23 April 2006
Available online 15 May 2006

Abstract

The origin of the low-energy emission of fluorene-based homo- and copolymers still remains controversial. In this work, the effect of thermal treatment on the emission properties of poly[(9,9-dihexylfluorene)-*alt*-co-(1,4-phenylene)] (PF6P) and its four derivatives modified by attaching different lengths of alkoxy side chains on the phenylene rings has been systematically investigated. By comparing the photoluminescence (PL) spectra of PF6P and the modified polymers, Fourier-transform infrared (FTIR) spectroscopy, X-ray diffraction (XRD) and PL lifetime measurements have revealed that the long wavelength emission could be attributed to the formation of fluorenone-based excimers rather than to the localized fluorenone π–π* transition, the energy transfer from fluorene segments to the fluorenone moieties, or the fluorenone defects generated by thermal oxidation during thermal treatment. Compared with PF6P, the attachment of alkoxy side chains on the phenylene rings effectively inhibits the aggregation of backbone chains, thus restrains the formation of fluorenone-based excimers and remarkably improves thermal stability of the spectra.

Keywords: Thermal treatment; Photophysical properties; Excimer

1. Introduction

As a kind of promising blue-light-emitting materials, fluorene-based conjugated polymers have been attracted extensive attention in the past decade due to their high photoluminescence efficiency and charge-carrier mobility, good processability and thermal stability, and tunability of photophysical properties [1–6]. In addition, as a host material, polyfluorenes (PFs) can enable full color (blue, green, and red) via energy transfer to longer wavelength emitters in blends with other conjugated polymers and with phosphorescent dyes [7–9]. PF homopolymers and copolymers usually exhibit liquid crystal phase [10–14], and can be oriented for fabricating highly polarized light emitting diodes (LEDs) [15,16]. However, PFs still cannot satisfy the requirements of commercial application of LEDs due to lifetime, spectral stability and other problems. In order to solve these problems, numerous efforts have been made by chemistry and physical approaches, such as structural modification or design of materials (e.g. using side chain substitution and copolymerization methods) and optimization of diode structures and encapsulation of diodes [17–19].

As is known, PFs are promising materials for the fabrication of polymer light-emitting diodes (PLEDs). However, these PLEDs fabricated from PF-based materials suffer from a degradation of the device under operation, most probably due to the formation of a low-energy emission band at 2.2–2.4 eV, as well documented in the literature [20,21]. As a result, the desired blue emission turns into the undesired long wavelength (blue–green and even yellow) emission to some extent. This low-energy emission of PFs is also observed in the photoluminescence (PL) [21–23] and the electroluminescence (EL) [24,25] spectra after thermal treatment. Extensive studies have been carried out and several possible explanations have been proposed in the past years regarding the formation mechanisms of the low-energy emission. Initially, the undesired long wavelength emission bands have usually been attributed to aggregate or excimer formation in the bulk materials [3,22–31]. And the formation of the excimers exhibits temperature and

* Corresponding author. Address: Key Laboratory of Molecular Engineering of Polymers of Chinese Ministry of Education, Department of Macromolecular Science, Institute of Advanced Materials, Fudan University, 220, Handan Road, Shanghai 200433, People's Republic of China. Tel.: +86 21 55664197; fax: +86 21 55664192.
E-mail address: txliu@fudan.edu.cn (T. Liu).

0032-3861/$ - see front matter © 2006 Elsevier Ltd. All rights reserved.
doi:10.1016/j.polymer.2006.04.056

concentration dependences. In other studies, however, the low-energy emission bands are assigned to the emission from fluorenone keto defects due to oxidation at the methane bridge [20,32–35]. The fluorenone moieties can trap singlet excitons and thus reduce PL efficiency. Yet, the formation mechanism of long wavelength emission from fluorenone keto defects also remains controversial. Scherf et al. proposed that the long wavelength emission for photo-oxidized poly(9,9-dioctylfluorene) was originated from monomeric fluorenone charge-transfer (CT) π–π* state [36]. Jenekhe et al. investigated four statistical copolymers containing 1, 3, 5 and 10% fluorenone and fluorene–fluorenone–fluorene trimer model compounds. Their results suggested that the long wavelength emission band was originated from fluorenone defects in single-chain polyfluorenes. And they proposed that the increased intensity of the green emission with the increase of intermolecular interaction in solution or solid state was due to the increased energy transfer from fluorene segments to the fluorenone moieties [37]. However, Bradley et al. suggested that the presence of fluorenone defects alone might not be sufficient to produce the green emission, and they attributed the long wavelength emission band to emission from fluorenone-based excimers [38]. Recently, the third interpretation on this undesirable long wavelength emission has been suggested, that is, the long wavelength emission could be attributed to the microscopic morphology of the films [39,40]. Hitherto, the exact origin(s) of the long wavelength emission bands remains not being fully understood. Therefore, it is important to identify the origin of the long wavelength emission bands and to in-depth understand the mechanism of the color degradation.

In this work, the photophysical properties of a series of fluorene-*alt*-benzene polymers with different lengths of alkoxy side chains on the phenylene rings were studied. The effects of annealing temperature, atmosphere, and side chain length on the optical properties of the polymer films were systematically investigated. And the origin of long wavelength emission of fluorene-based polymers was discussed.

2. Experimental

2.1. Materials

The chemical structures of the copolymers used in the present study are shown in Scheme 1. Poly[(9,9-dihexylfluorene)-*alt*-co-(1,4-phenylene)] (PF6P), poly[(9,9-dihexylfluorene)-*alt*-co-(2,5-dihexyloxy-1,4-phenylene)] (PF6OC6), poly[(9,9-dihexylfluorene)-*alt*-co-(2,5-dioctyloxy-1,4-phenylene)] (PF6OC8), poly[(9,9-dihexylfluorene)-*alt*-co-(2,5-didecyloxy-1,4-phenylene)] (PF6OC10), and poly[(9,9-dihexylfluorene)-*alt*-co-(2,5-didodecyloxy-1,4-phenylene)] (PF6OC12) were prepared from 9,9-dihexylfluorene-2,7-bis(trimethylene boronate) and 1,4-dibromobenzene or the corresponding 1,4-dibromo-2,5-bisalkoxybenzenes through Suzuki coupling reaction, as described in the literature [4]. The structures of the polymers were confirmed by ^{1}H and ^{13}C NMR and elemental analysis.

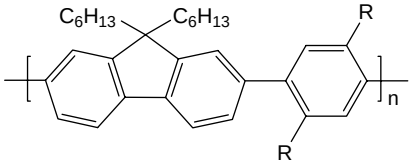

R = H	PF6P
OC_6H_{13}	PF6OC6
OC_8H_{17}	PF6OC8
$OC_{10}H_{21}$	PF6OC10
$OC_{12}H_{25}$	PF6OC12

Scheme 1. Chemical structures of the copolymers used.

Poly[(9,9-dihexylfluorene)-*alt*-co-(1,4-phenylene)] (PF6P). Cyan powder. ^{1}H NMR (400 MHz, $CDCl_3$): δ (ppm) 7.84–7.65 (8H, m), 7.24 (2H, s), 2.04 (4H, s), 1.07–0.75 (22H, m). ^{13}C NMR (100 MHz, $CDCl_3$): δ (ppm) 151.71, 145.46, 140.42, 140.05, 139.55, 127.48, 125.84, 121.36, 120.02, 55.44, 31.61, 30.05, 25.57, 22.92, 16.68, 14.33. Anal. Calcd for $C_{31}H_{36}$: C, 91.18; H, 8.82. Found: C, 91.00; H, 8.95.

Poly[(9,9-dihexylfluorene)-*alt*-co-(2,5-dihexyloxy-1,4-phenylene)] (PF6OC6). ^{1}H NMR (400 MHz, $CDCl_3$): δ (ppm) 7.83–7.79 (d, 2H), 7.74 (s, 2H), 7.61–7.56 (d, 2H), 7.14 (s, 2H), 4.03–3.97 (t, 4H), 2.18 (s, 4H), 1.81–1.67 (m, 4H), 1.39–0.76 (m, 40H). ^{13}C NMR (100 MHz, $CDCl_3$): δ (ppm) 150.78, 140.11, 137.27, 131.49, 127.17, 124.67, 119.44, 117.05, 70.14, 55.31, 40.81, 32.04, 31.95, 30.25, 29.72, 26.38, 24.28, 22.98, 22.91, 14.24. Anal. Calcd for $C_{43}H_{60}O_2$: C, 84.81; H, 9.93; O, 5.25. Found: C, 84.76; H, 9.91; O, 5.14.

Poly[(9,9-dihexylfluorene)-*alt*-co-(2,5-dioctyloxy-1,4-phenylene)] (PF6OC8). ^{1}H NMR (400 MHz, $CDCl_3$): δ (ppm) 7.81–7.78 (d, 2H), 7.72 (s, 2H), 7.59–7.56 (d, 2H), 7.13 (s, 2H), 4.00–3.96 (t, 4H), 2.04 (s, 4H), 1.76–1.71 (m, 4H), 1.40–0.76 (m, 48H). ^{13}C NMR (100 MHz, $CDCl_3$): δ (ppm) 150.78, 140.10, 137.26, 131.50, 128.18, 124.68, 119.47, 117.02, 70.14, 55.30, 40.82, 32.06, 31.96, 30.25, 29.75, 29.59, 29.55, 26.37, 24.28, 22.98, 22.91, 14.35, 14.28. Anal. Calcd for $C_{47}H_{68}O_2$: C, 84.88; H, 10.33; O, 4.81. Found: C, 84.78; H, 10.19; O, 4.74.

Poly[(9,9-dihexylfluorene)-*alt*-co-(2,5-didecyloxy-1,4-phenylene)] (PF6OC10). ^{1}H NMR (400 MHz, $CDCl_3$): δ (ppm) 7.82–7.79 (d, 2H), 7.72 (s, 2H), 7.60–7.57 (d, 2H), 7.14 (s, 2H), 4.01–3.97 (t, 4H), 2.03 (s, 4H), 1.77–1.72 (m, 4H), 1.41–0.76 (m, 56H). ^{13}C NMR (100 MHz, $CDCl_3$): δ (ppm) 150.77, 140.10, 137.27, 131.49, 128.18, 124.70, 119.48, 117.00, 70.12, 55.30, 40.87, 32.15, 31.96, 30.25, 29.93, 29.82, 29.74, 29.60, 26.37, 24.28, 22.99, 22.93, 14.37, 14.29. Anal. Calcd for $C_{51}H_{76}O_2$: C, 84.94; H, 10.62; O, 4.44. Found: C, 84.83; H, 10.48; O, 4.35.

Poly[(9,9-dihexylfluorene)-*alt*-co-(2,5-didodecyloxy-1,4-phenylene)] (PF6OC12). ^{1}H NMR (400 MHz, $CDCl_3$): δ (ppm) 7.82–7.79 (d, 2H), 7.73 (s, 2H), 7.61–7.58 (d, 2H), 7.13 (s, 2H), 4.00–3.95 (t, 4H), 2.04 (s, 4H), 1.77–1.72 (m, 4H), 1.42–0.75 (m, 64H). ^{13}C NMR (100 MHz, $CDCl_3$): δ (ppm) ^{13}C NMR (100 MHz): δ (ppm) 150.79, 140.11, 137.30, 131.50, 128.17, 124.70, 119.50, 117.00, 70.12, 55.32, 40.89, 32.19, 31.99, 30.29, 29.97, 29.92, 29.89, 29.76, 29.63, 26.39, 24.24, 23.01, 22.96, 14.39, 14.31. Anal. Calcd for $C_{55}H_{84}O_2$: C, 84.99; H, 10.89; O, 4.12. Found: C, 84.85; H, 10.73; O, 4.03.

2.2. Sample preparation and characterization

^{1}H and ^{13}C NMR spectra were recorded on Varian Mercury Plus 400 spectrometer in deuterated chloroform solution at ambient temperature with tetramethylsilane as the internal standard. Elemental analyses were carried out on a Vario EL III CHNOS Elementar analyzer. Number-average (M_n) and weight-average (M_w) molecular weights were determined by gel permeation chromatography (GPC) with a HP1100 HPLC system equipped with 7911GP-502 and GP NXC columns (as shown in Table 1). The calibration was made with a series of monodispersed polystyrene standards in THF.

All thin films of the copolymers for optical (UV–vis absorption and PL) characterization were prepared by spin-coating onto quartz substrates from 6 mg mL^{-1} chloroform solution. UV–vis absorption spectra were recorded on Shimadzu 3150 PC spectrophotometer and fluorescence measurement was carried out on Shimadzu RF-5301 PC spectrofluorometer with a xenon lamp as a light source.

Samples for Fourier-transform infrared (FTIR) spectroscopy measurements were prepared by drop-casting the chloroform solution onto the pressed, anhydrous KBr pellets. FTIR spectra were then recorded from 500 to 3500 cm^{-1} using a Shimadzu IR Prestige-21 spectrometer with a resolution of 1 cm^{-1}. The thermal treatment of all film samples was carried out in a glass oven in air or nitrogen atmospheres.

Photoluminescence quantum efficiency (PLQE) measurements were made using a calibrated integrating sphere coupled via an optical fiber linked to a scanning monochromator with a photomultiplier detector. The samples were excited with the 374 nm Zolix PHLM-2 laser. PL lifetime measurements were performed using an Edinburgh Lifespec-ps with an f900 system.

X-ray diffraction (XRD) measurements were carried out for the powdery polymer samples using a Bruker Nanostar U System, with incident X-ray wavelength ($\lambda = 0.1542$ nm) at room temperature. The collimation system consists of two cross-coupled Gobel Mirrors and 4 pinholes. A Histar 2D area detector (Siemens) filled with pressurized xenon gas was used to record the one-dimensional (1D) XRD scattering patterns at voltage of 40 kV and current of 40 mA.

3. Results and discussion

Figs. 1 and 2(a) show the UV–vis absorption and PL spectra of PF6P (without the alkoxy side chain on the phenylene rings) thin films, respectively, annealed in air at the indicated temperatures. PF6P exhibits the absorption maximum at about 376 nm (Fig. 1). Its PL emission spectral peak was observed at 422 nm with a distinct shoulder peak at 440 nm and another discriminable shoulder around 473 nm (Fig. 2(a)). The emission spectra indicate the presence of well-defined vibronic structures. It can be seen that with increasing the annealing temperature, the PL intensity of the long wavelength (greenish) band around 515 nm steadily increases and the UV–vis

Table 1
Molecular weights of the polymers synthesized

Polymer	M_n	M_w	M_w/M_n
PF6P	7188	9970	1.39
PF6OC6	17,543	27,985	1.60
PF6OC8	22,262	39,862	1.79
PF6OC10	29,414	53,829	1.83
PF6OC12	19,974	36,153	1.81

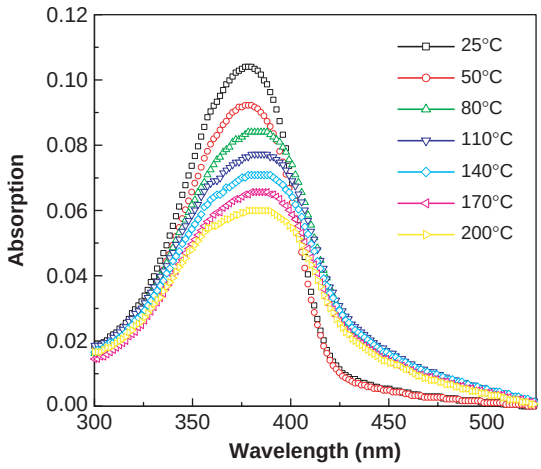

Fig. 1. UV–vis absorption spectra of PF6P films annealed at different temperatures for 1 h in air.

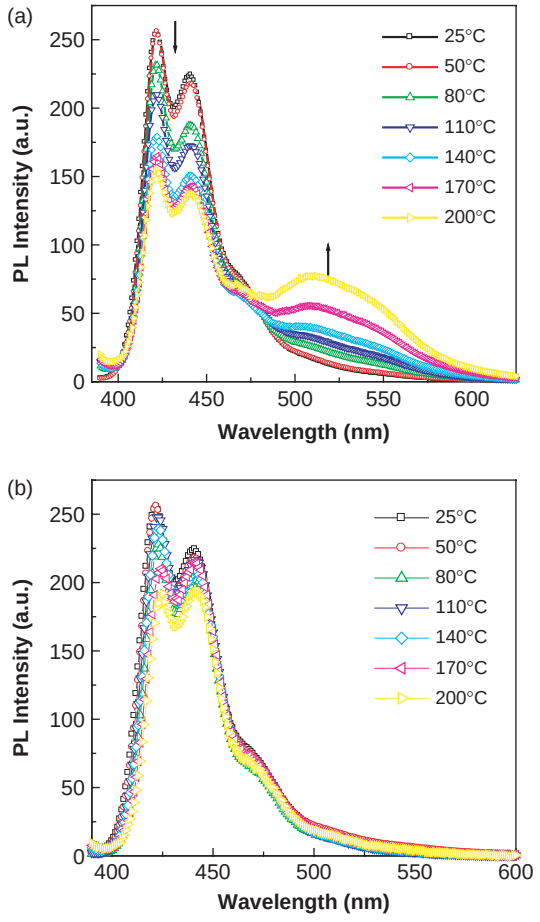

Fig. 2. Photoluminescence (PL) spectra of PF6P films annealed at different temperatures for 1 h in air (a) and in nitrogen (b) atmospheres.

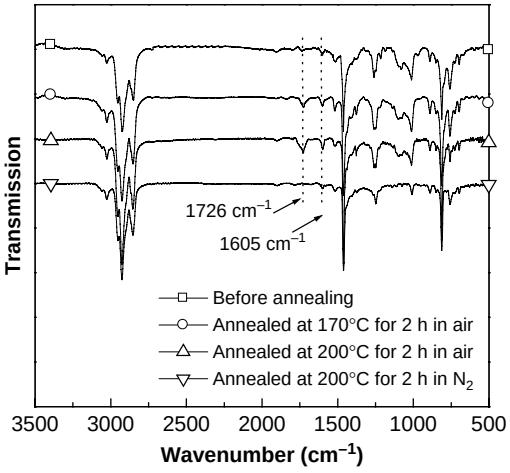

Fig. 3. FTIR spectra of the as-cast PF6P film and the films annealed at different conditions.

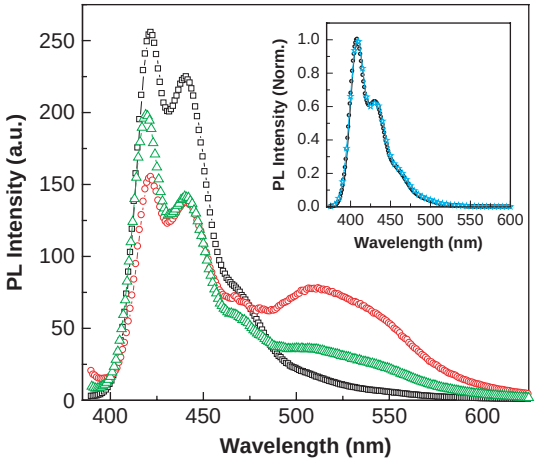

Fig. 4. PL spectra of different PF6P films: the pristine film (squares), the film annealed at 200 °C for 1 h in air (circles), and the film, which was cast from chloroform solution of the annealed polymer at 200 °C for 1 h in air (triangles). The inset is PL spectra of two chloroform solutions prepared from the pristine polymer and the polymer annealed at 200 °C for 1 h in air, respectively.

absorption peak gradually broadens, which is consistent with the results observed in other fluorene-based polymers [21,22,25]. The long wavelength PL emission was previously attributed to aggregate and/or excimer formation in the bulk materials [3,22–30]. However, the PL spectra did not change when the films were annealed at different temperatures in nitrogen atmosphere (as shown in Fig. 2(b)). The spectral difference of the films annealed in the air and nitrogen atmosphere indicated that the long wavelength emission could not be attributed to aggregate and/or excimer formation.

In order to probe the structural changes of PF6P films before and after thermal treatment, FTIR was used to measure the transmission spectra of the pristine PF6P film and the films annealed at different conditions, as shown in Fig. 3. An IR absorption peak at 1726 cm^{-1} is observed for the films annealed in air, and its intensity gradually increases with increasing annealing temperature. The position of the 1726 cm^{-1} band is consistent with the known IR spectrum of fluorenone (not shown here). The peak located at 1605 cm^{-1} is related to phenyl/phenylene ring vibrations, and its intensity is very weak in pristine PF6P film and the annealed PF6P film in nitrogen atmosphere, but it also exhibits slight temperature dependence in the PF6P films annealed in the air. The increasing intensity of 1726 cm^{-1} band is also consistent with the formation of fluorenone. However, we did not observe any absorption peak at 1726 cm^{-1} in the pristine PF6P film and the films annealed in nitrogen atmosphere. Thus, it could be concluded that the fluorenone defects (with two characteristic IR absorption peaks at 1726 and 1605 cm^{-1}) were introduced during the thermal treatment of the PF6P films because of thermal oxidization in the air. And, the long wavelength emission bands (Fig. 2(a)) and the IR absorption bands (Fig. (3)) show similar temperature dependence, which suggests that the presence of long wavelength emission is closely related to the formation of fluorenone defects upon thermal oxidation or treatment in the air.

As shown in Fig. 4, for the PF6P film (indicated by circles) annealed at 200 °C for 1 h in the air, the long wavelength emission band was clearly observed, compared with the pristine film (indicated by squares). For comparison, here the polymer film annealed at 200 °C for 1 h in air was re-dissolved in chloroform and re-cast into film. And, the PL spectrum of the re-cast film was shown in Fig. 4, as indicated by triangles. The long wavelength emission of the re-cast film was observed and located between those of the pristine and the annealed films. Interestingly, however, the PL spectrum (the inset of Fig. 4) of chloroform solution of the polymer annealed at 200 °C in air is completely identical with that of pristine polymer without any thermal treatment. The above experiments indicated that the long wavelength emission of PF6P was not originated from monomeric fluorenone defect because it was not observed in chloroform solution of the annealed polymer in the air (see the inset of Fig. 4). The main difference between the two samples (i.e. the annealed PF6P film and the chloroform solution of the annealed polymer) is the intermolecular interaction in film and solution states. In general, the intermolecular interaction in dilute solution is very weak and can usually be neglected. Therefore, we considered that the long wavelength emission of annealed PF6P films was probably related to the intermolecular interaction of fluorenone moieties generated during thermal oxidation.

Fig. 5 shows the UV–vis absorption and PL spectra of PF6OC6, PF6OC8, PF6OC10 and PF6OC12 films. The four polymers have the same backbone structures as PF6P, and the only structural difference among them is the length of the alkoxy side chains on the phenylene rings, and. PF6OC6 exhibits the absorption maximum at 382 nm and the PL emission maximum at 420 nm. When the substituent is changed (i.e. increased) from hexyloxy group (PF6OC6) to dodecyloxy group (PF6OC12), the UV–vis absorption and PL spectra of the polymers are very close to those obtained for PF6OC6 as the conformational effect of alkoxy side chains on spectroscopic properties of the polymers is small [41]. The PL spectra of the four polymers films are also similar to that of PF6P, and only 2 nm blue-shift is observed, which can be

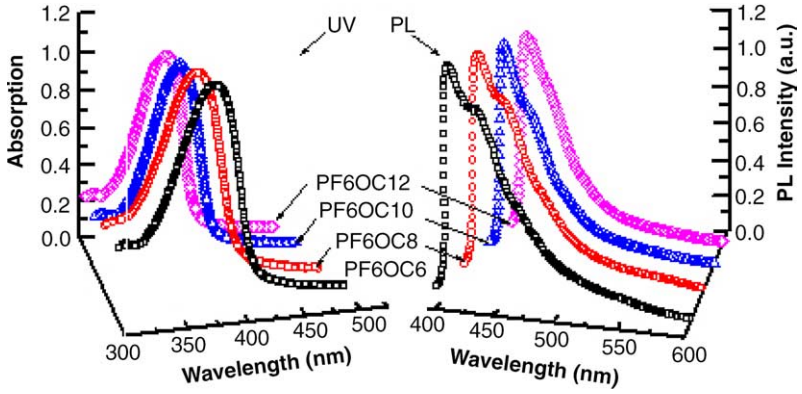

Fig. 5. UV–visible absorption and PL spectra of PF6OC6, PF6OC8, PF6OC10 and PF6OC12 films, as a function of alkoxy side chain length.

attributed to the alkoxy property of being a weakly electronic donor. Moreover, the vibronic structures (with a characteristic shoulder around 440 nm) in PL spectra were gradually and remarkably reduced (or inhibited) with increasing the length of substituted alkoxy side chains on the phenylene ring of PF6P. We consider that the decrease of the shoulder peak at about 440 nm for the vibronic structures in PL spectra is probably related to film morphology of the polymers. Detailed studies about this specific topic are under investigations in our lab.

Similar annealing experiments in the air were also carried out for the four substituted polymers, and here only the results for PF6OC6 were given and discussed as an example. Fig. 6 shows the PL spectra of PF6OC6 films annealed in the air at the indicated temperatures. In contrast to the case of PF6P, the long wavelength emission at about 515 nm was surprisingly not observed in the PL spectra of the annealed PF6OC6 films. It indicates that the hexyloxy substitution on the phenylene rings almost completely restrains the long wavelength emission, compared with that of PF6P. The structural change of the annealed PF6OC6 films was also characterized using FTIR and the transmission spectra of PF6OC6 films annealed at different conditions were shown in Fig. 7. Similar to PF6P, the absorption peak at 1726 cm^{-1} was observed in the spectra of the PF6OC6 films annealed in the air, but did not appear in the spectra of pristine PF6OC6 film and the PF6OC6 films annealed in nitrogen atmosphere. The absorption peak located at 1605 cm^{-1} was observed in pristine film and the annealed film in nitrogen atmosphere. And the intensity of the two absorption peaks also exhibited temperature dependence for the PF6OC6 films annealed in the air. That is, the intensity of the absorption peaks increases with increasing the annealing temperature in the air. Therefore, it can be concluded that the PF6OC6 films were oxidated and fluorenone defects were also generated during the thermal treatment in the air.

Although the annealing experiments for both the films of PF6P and PF6OC6 are identical and generate the fluorenone defects in the annealed films, the PL spectra of the two polymer films exhibit remarkable difference (see Figs. 2(a) and 6). That is, the long wavelength emission was not observed in the annealed PF6OC6 films. This suggests that the long wavelength emission band for PF6P is not originated from the monomeric fluorenone CT π–π* transition and energy transfer from fluorene segments to the fluorenone moieties. Thus, we consider that the long wavelength emission for PF6P films annealed in the air is originated from fluorenone-based excimers. The hexyloxy substitution on the phenylene rings (i.e. for PF6OC6) may effectively separate the molecular backbone chains in all three dimensions and thus restrain the formation of excimers. Therefore, the long wavelength

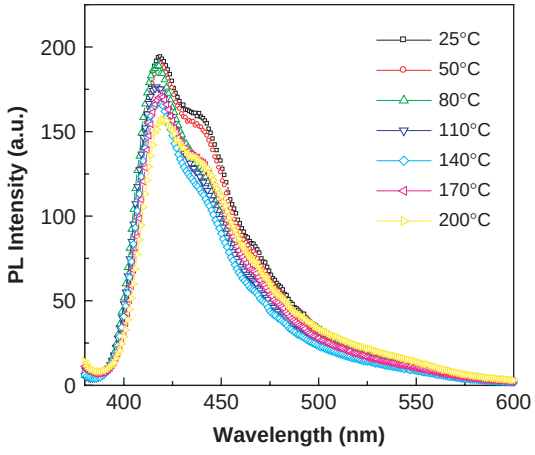

Fig. 6. PL spectra of PF6OC6 films annealed at different temperatures for 1 h in air.

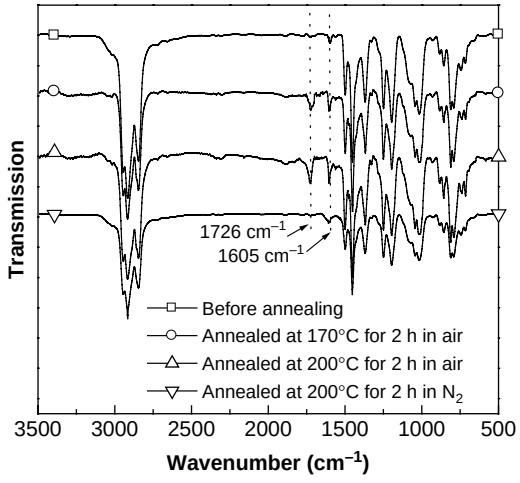

Fig. 7. FTIR spectra of the as-cast PF6OC6 film and the films annealed at different conditions.

emission of annealed PF6OC6 films could not be observed. These will be further demonstrated in the following investigations.

An excimer is a pair of two molecules whose interaction is repulsive in the ground state but attractive if one of the molecules is excited. The basic supramolecular structure of an excimer is a cofacial sandwich-type configuration. Typically the separation of the molecules is about 0.3–0.4 nm [23,38,42,43]. At larger distances the attractive interaction, which arises from the overlap of the π electrons, is very weak, and at smaller distances the repulsion due to closed shells dominates. That means that excimer formation is a result of short distance intermolecular interaction. The XRD spectra of PF6P, PF6OC6, PF6OC8, PF6OC10 and PF6OC12 are shown in Fig. 8. For PF6P, only a very broad and diffused scattering 'peak' was observed, indicating a disordered structure. However, for PF6OC6, PF6OC8, PF6OC10 and PF6OC12, the XRD patterns show very strong first-order reflections at angles of 6.67, 6.14, 5.48 and 5.00°, corresponding to the *d*-values of 1.33, 1.44, 1.61 and 1.77 nm, respectively. It indicates that, for the substituted PF6P derivatives, the reflection peaks shift toward lower 2θ angles with increasing the length of alkoxy side chains, thus corresponding to an increased interlayer spacing (as shown in the insert of Fig. 8). That is, the rigid-rod main chains are spaced by the flexible alkoxy side chains. However, the interlayer spacing is slightly shorter than the twice of the length of side chain, thus probably indicating the formation of an inter-digitated packing. The PF6P derivatives can, depending on the nature of side-chains, display different types of morphologies. Detailed studies of the effect of side chain on the morphology and thus photophysical properties will be reported separately. Obviously, alkoxy substitutions on the phenylene rings can effectively separate the backbone chains and remarkably increase the distance of packing between the polymer main chains. The distance between two backbone chains substituted with alkoxy side chains on the phenylene rings is much higher than the effective distance (0.3–0.4 nm) of forming excimers. The long wavelength emission can be observed in the annealed PF6P films (see Fig. 2(a)), but not appear in the annealed PF6OC6 films (see Fig. 6). Therefore, it can be concluded that the long wavelength emission of the annealed PF6P film is originated from the fluorenone-based excimers generated by thermal oxidation.

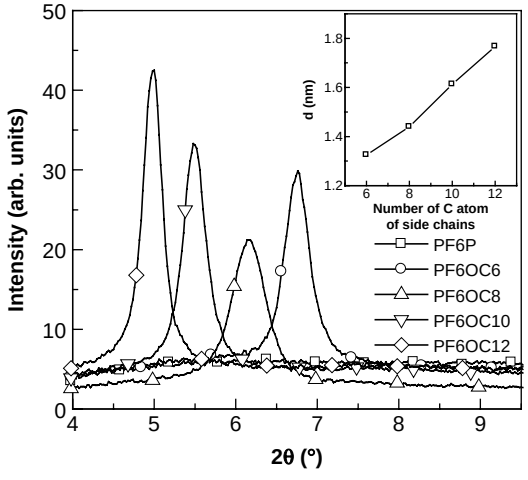

Fig. 8. XRD spectra of PF6P, PF6OC6, PF6OC8, PF6OC10 and PF6OC12. The inset is the distance of π–π stacking between the polymer main chains as a function of the length of side chain.

Fig. 9 shows the PL spectra of all the five polymer films annealed at 200 °C for 1 h in the air. Except for the PF6P film, the long wavelength emission was not observed in the annealed PF6OC8, PF6OC10 and PF6OC12 films, either, which is consistent with the results of PF6OC6. In addition, the spectral stability of the annealed polymer films exhibit slight length dependence of alkoxy side chains attached on phenylene rings. That is, the full width at the half-maximum of the PL spectra and the vibronic structures in the PL spectra gradually decrease with increasing the length of substituted alkoxy side chains on the phenylene rings, as observed for the pristine polymer films.

In general, the formation of excimers exhibits some particular optical properties. One characteristic of forming excimers is presence of a new emission peak being totally different from pristine emission band in the PL spectra of sample, and also the intensity of the new emission peak exhibits strong concentration dependence [44]. The present long wavelength emission of PF6P films annealed in the air is located at 515 nm and differs from the PL emission (422 nm) of the pristine film, and its intensity exhibits temperature dependence (i.e. concentration dependence of fluorenone defects generated during thermal treatment in the air, as indicated in Fig. 3), which is consistent with the above characteristic of excimers formation. Another characteristic of forming excimers is a long PL lifetime, because the transition of excimers is usually forbidden by symmetry [43]. Here, the transient PL decays for the annealed PF6P films were compared. Fig. 10 shows the PL decays for the intra-chain emission of a pristine PF6P film and the excimer emission of the annealed films at 170 and 200 °C in the air. Each decay curve was measured after being excited at 382 nm, and all the curves can be fitted with single exponentials. The PL lifetimes are 720, 1040 and 7300 ps for the pristine PF6P film, and the films annealed at 170 and 200 °C for l h in the air, respectively.

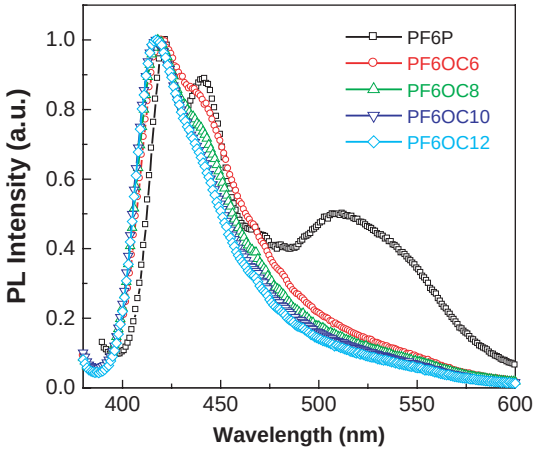

Fig. 9. PL spectra of PF6P, PF6OC6, PF6OC8, PF6OC10 and PF6OC12 films annealed at 200 °C for 1 h in air.

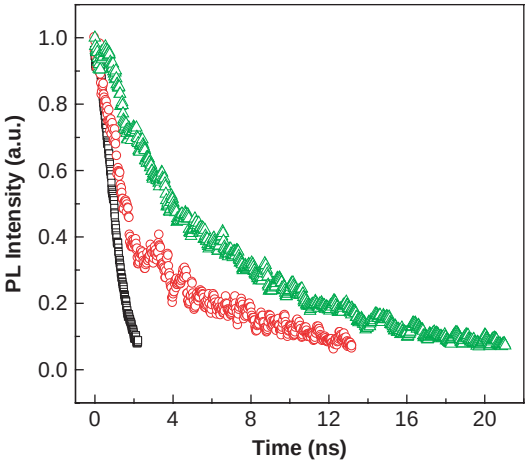

Fig. 10. Transient PL decay profiles for the intra-chain emission of pristine PF6P film (open square), for excimer emission of annealed films at 170 °C (open circle) and 200 °C (open triangle) for 1 h in air.

In addition, the decay time indicates that the PF6P film was heavily oxidized after being annealed at 200 °C for 1 h in the air. The decay time of the long wavelength emission in the annealed PF6P films is considerably longer than the normal intra-chain emission of the pristine PF6P film, which is also consistent with the above characteristic of the excimer formation. Therefore, the proposed origin of the long wavelength emission of the annealed PF6P films (i.e. from the fluorenone-based excimers) has further been confirmed.

The structural modification for PF6P by attaching alkoxy side chains on the phenylene rings almost does not affect the PL emission of the substituted polymers and thus remarkably improves the thermally spectral stability of the modified polymers (PF6OC6, PF6OC8, PF6OC10 and PF6OC12), compared with that of PF6P. An additional investigation on photoluminescence quantum efficiency (PLQE) has been performed to further compare the optical property between the modified polymers and PF6P. Fig. 11 shows the PLQE of all pristine polymer films (the insert) and the PF6P and

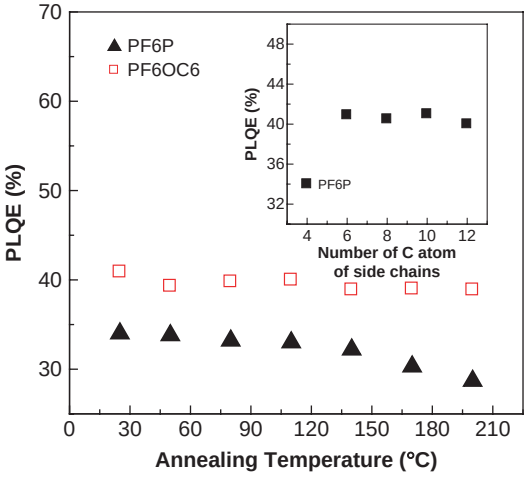

Fig. 11. Photoluminescence quantum efficiency (PLQE) of PF6P and PF6OC6 films annealed at different temperatures for 1 h in air. The inset is the PLQE of pristine PF6P, PF6OC6, PF6OC8, PF6OC10 and PF6OC12 films.

PF6OC6 films annealed at different temperatures for 1 h in the air. The PLQE of the polymers with alkoxy substitutions on the phenylene rings is about $40 \pm 1\%$ (the inset of Fig. 11), and the further increase of alkoxy side chain length does not have obvious effect on the PLQE of the modified polymers. And the PLQE (about 40%) of the substituted polymers is higher than that of PF6P (34%), which can be attributed to the electronic donor property of the alkoxy side chains. Moreover, it can be observed that the PLQE of the annealed PF6P films steadily decreases with increasing the annealing temperature, due to an increasing quenching effect with the temperature by the formation/presence of fluorenone generated during thermal oxidation. However, the PLQE of the annealed PF6OC6 films remains almost constant with increasing the annealing temperature, indicating that the alkoxy side chains on the phenylene rings can restrain the quenching effect of fluorenone, by effectively separating the packing in space between the polymer main chains. Thus, the alkoxy side chains play an important role in improving the thermally spectral stability of the polymers.

4. Conclusions

In summary, the effect of thermal treatments on the PL spectra of poly[(9,9-dihexylfluorene)-*alt*-co-(1,4-phenylene)] (PF6P) has been systematically investigated. The results of FTIR measurements show that the long wavelength emission of the annealed PF6P films is closely related to the fluorenone defects generated by thermal oxidation. Another four polymers (PF6OC6, PF6OC8, PF6OC10 and PF6OC12) modified by attaching different lengths of alkoxy side chains on the phenylene rings of PF6P are used for the purpose of comparison. By comparing the PL spectra between PF6P and the modified polymers, the long wavelength emission of the annealed PF6P films is assigned to the fluorenone-based excimers formed during thermal treatment in the air. The proposed origin of the long wavelength emission has been further confirmed by XRD and PL lifetime characterizations. The XRD experiments reveal that the distance of π–π stacking between the main chains of the modified polymers increases by the alkoxy substitutions on the phenylene rings, and thus greatly restrains the formation of excimers in the annealed substituted polymers. Moreover, the PLQE measurements indicate that the alkoxy side chains on the phenylene rings effectively restrain the quenching effect from the fluorenone defects, compared with PF6P. Therefore, the alkoxy side chains play an important role in effectively separating the molecular backbones, and in restraining the formation of excimers, thus remarkably improving the thermally spectral stability of the modified polymers.

Acknowledgements

This work was financially supported by the National Natural Science Foundation of China (Grant No. 50403012), the 'Program for New Century Excellent Talents (NCET) in

University' (Grant No. NCET-04-0355), and the 'Shanghai Rising-Star Program' (Grant No. 04QMX1403).

References

[1] Pei Q, Yang Y. J Am Chem Soc 1996;118(31):7416.
[2] Yang Y, Pei Q. J Appl Phys 1997;81(7):3294.
[3] Kreyenschmidt M, Klaerner G, Fuhrer T, Ashenhurst J, Karg S, Chen WD, et al. Macromolecules 1998;31(4):1099.
[4] Liu B, Yu WL, Lai YH, Huang W. Chem Mater 2001;13(6):1984.
[5] Jin SH, Kim MY, Koo DS, Kim YI, Park DH, Lee K, et al. Chem Mater 2004;16(17):3299.
[6] Wu FI, Shih PI, Shu CF, Tung YL, Chi Y. Macromolecules 2005;38(22): 9028.
[7] Buckley AR, Rahn MD, Hill J, Cabanillas-Gonzalez J, Fox AM, Bradley DDC. Chem Phys Lett 2001;339:331.
[8] O'Brien DF, Giebeler C, Fletcher RB, Cadby AJ, Palilis LC, Lidzey DG, et al. Synth Met 2001;116:379.
[9] Gong X, Ostrowski JC, Bazan GC, Moses D, Heeger AJ, Liu MS, et al. Adv Mater 2003;15:45.
[10] Grell M, Bradley DDC, Inbasekaran M, Woo EP. Adv Mater 1997;9:798.
[11] Neher D. Macromol Rapid Commun 2001;22:1366.
[12] Teetsov JA. Vanden Bout DA. J Am Chem Soc 2001;123(15):3605.
[13] Kawana S, Durrell M, Lu J, Macdonald JE, Grell M, Bradley DDC, et al. Polymer 2002;43:1907.
[14] Chen SH, Su AC, Su CH, Chen SA. Macromolecules 2005;38(2):379.
[15] Virgili T, Lidzey DG, Grell M, Walker S, Asimakis A, Bradley DDC. Chem Phys Lett 2001;341:219.
[16] Misaki M, Ueda Y, Nagamatsu S, Yoshida Y, Tanigaki N, Yase K. Macromolecules 2004;37(18):6926.
[17] Wong WY, Liu L, Cui D, Leung LM, Kwong CF, Lee TH, et al. Macromolecules 2005;38:4970.
[18] Chan LH, Lee RH, Hsieh CF, Yeh HC, Chen CT. J Am Chem Soc 2002; 124:6469.
[19] Alvaro M, Corma A, Ferrer B, Galletero MS, Garcia H, Peris E. Chem Mater 2004;16:2142.
[20] Gaal M, List EJW, Scherf U. Macromolecules 2003;36(11):4236.
[21] Gong X, Iyer PK, Moses D, Bazan GC, Heeger AJ, Xiao SS. Adv Funct Mater 2003;13:325.
[22] Bliznyuk VN, Carter SA, Scott JC, Klärner G, Miller RD, Miller DC. Macromolecules 1999;32(2):361.
[23] Zeng G, Yu WL, Chua SJ, Huang W. Macromolecules 2002;35(18):6907.
[24] Uckert F, Tak YH, Müllen K, Bässler H. Adv Mater 2000;12:905.
[25] Weinfurtner KH, Fujikawa H, Tokito S, Taga Y. Appl Phys Lett 2000;76: 2502.
[26] Lemmer U, Hem S, Mahrt RF, Scherf U, Hopmeier M, Siegner U, et al. Chem Phys Lett 1995;240:373.
[27] Lee JI, Llaerner, Miller RD. Chem Mater 1999;11(4):1083.
[28] Teetsov J, Fox MA. J Mater Chem 1999;9:2117.
[29] Silva C, Russell DM, Dhoot AS, Herz LM, Daniel C, Greenham NC, et al. Phys Cond Matt 2002;14:9803.
[30] Jacob J, Oldridge L, Zhang J, Gal M, List EJW, Grimsdale AC, et al. Curr Appl Phys 2004;4:339.
[31] Zhou CZ, Liu TX, Lin TT, Zhan XH, Chen ZK. Polymer 2005;46:10952.
[32] Scherf U, List EJW. Adv Mater 2002;14:477.
[33] Gamerith S, Gadermaier C, Scherf U, List EJW. Phys Stat Sol 2004;201: 1132.
[34] Romaner L, Pogantsch A, Freitas PSD, Scherf U, Gaal M, Zojer E, et al. Adv Funct Mater 2003;13:597.
[35] List EJW, Guentner R, de Freitas PS, Scherf U. Adv Mater 2002;14:374.
[36] Zojer E, Pogantsch A, Hennebicq E, Beljonne D, Brédas JL, Freitas PS, et al. Chem Phys 2002;117:6794.
[37] Kulkarni AP, Kong X, Jenekhe SA. J Phys Chem B 2004;108:8689.
[38] Sims M, Bradley DDC, Ariu M, Koeberg M, Asimakis A, Grell M, et al. Adv Funct Mater 2004;14:765.
[39] Surin M, Hennebocq E, Ego C, Marsitzky D, Grimsdale AC, Müller K, et al. Chem Mater 2004;16:994.
[40] Chochos CL, Tsolakis PK, Gregorious VG, Kallitsis JK. Macromolecules 2004;37:2502.
[41] Kato H, Karatsu T, Kaito A, Matsuyama S, Kitamura A. Polymer 2003; 44:3269.
[42] Jenekhe SA, Osaheni JA. Science 1994;265:765.
[43] Conwell EM. Synth Met 1997;85:995.
[44] Huang CH, Li FY, Huang YY. Ultrathin films for optics and electronics. Beijing: Beijing University Press; 2001.